CIRP Annals - Manufacturing Technology 74 (2025) 339–343

Contents lists available at ScienceDirect

CIRP Annals - Manufacturing Technology

journal homepage: https://www.editorialmanager.com/CIRP/default.aspx

Exploring the feasibility of a closed-loop industrial symbiosis link through Friction Stir Extrusion-based Additive Manufacturing

Kirill Kalashnikov, Davide Campanella, Giuseppe Ingarao, Gianluca Buffa, Livan Fratini (1)*, Fabrizio Micari (1)

Department of Engineering, University of Palermo, Viale delle Scienze 90128, Palermo, Italy

ARTICLE INFO

Article history:
Available online 13 May 2025

Keywords:
Additive manufacturing (am)
Recycling
Friction stir welding

ABSTRACT

A novel approach combining friction stir extrusion-based chips recycling and additive manufacturing was investigated to assess its suitability for a closed-loop industrial symbiosis. Recycled wires made from heat-treatable aluminum alloy AA6082 were used as a feedstock for solid-state additive manufacturing. The macrostructure and microstructure of the material were analyzed to reveal the layer formation mechanics and their influence on the micro and macro mechanical properties of the build. The produced material is characterized by a unique temper providing mechanical properties close to AA6082-T4. Finally, the proposed approach was compared with competitive technologies in terms of deposition rate and energy consumption.

© 2025 The Author(s). Published by Elsevier Ltd on behalf of CIRP. This is an open access article under the CC BY license (http://creativecommons.org/licenses/by/4.0/)

1. Introduction

At present, aluminum alloys are one of the most important materials in different industries. About 40 % of all industrial metals mined worldwide account for aluminum [1]. Aluminum and its alloys are widely used for civil engineering, aerospace, marine, and other applications [2].

In recent years, metal additive manufacturing (AM) has grown considerably in different industrial applications. However, all the most developed technologies are based on fusion welding [3], and additive manufacturing of aluminum alloys is accompanied by high porosity and hot-cracking, as in the case of laser powder-bed fusion of high-strength alloy AA2024 [4]. Despite that, during the last few years, among fusion-based techniques wire-arc additive manufacturing (WAAM) has become more suitable for aluminum alloys due to the development of Cold Metal Transfer technology [5]. A few papers can be found in the literature showing the possibility of 3D printing using heat-treatable filler wires made of AA2319 and AA6063; however, the results still show high porosity levels [6,7]. More than that, other alloys of these series are usually not available in the form of wire [8]. Due to limited ductility in the heat-treated state, the sensitivity of these alloys to thermal history, and their tendency to crack, it is still challenging to produce wires from heat-treatable aluminum alloys.

To avoid these limitations and the typical problems related to material melting, friction-based additive manufacturing techniques have been adopted [9]. Additive friction stir deposition (AFSD) is the most developed technology to date. The process has been proven to be suitable for producing components made of different aluminum alloys [10]. However, AFSD requires dedicated machines to provide the additional feeding axis, and in this case, there could be some limitations connected with the product geometry caused by the equipment. In contrast with AFSD, Multi-Layer Friction Surfacing (MLFS) does not require dedicated machines, although it also shows high suitability for aluminum alloy additive manufacturing. However, this method is accompanied by a high level of material waste connected with the usage of consumable tools [11].

For these reasons, new technologies competitive to AFSD and MLFS, based on the friction stir extrusion process, are under development. These processes can operate with a feedstock in the form of wire, rod, powder, and other types. Being this technology in its early stage of development, only an extremely limited number of papers can be found in the literature, corresponding to two different approaches: the so-called wire-based friction stir additive manufacturing [12] and friction screw extrusion additive manufacturing [13]. T. Bor et al. [14] showed the friction screw extrusion additive manufacturing process using AA6060 alloy. The authors declare the good suitability of such a technology for the additive manufacturing of aluminum alloy components despite decreased mechanical properties due to thermomechanical action during the deposition. Also, the SolidStir extrusion technology was suggested in work [15] as a solution suitable for wire- or rod-based deposition. However, there are remaining problems connected with the production of feedstock made of heat-treatable alloys. In the case of AFSD technology, a promising way is to produce rods by pressing aluminum chips, as shown in [16]. Unfortunately, this approach has some specific problems such as the low density of the resulting feedstock [16]. As a possible solution to the feedstock issue for wire-based methods, friction stir extrusion technology can be used [17]. This method is based on the solid-state recycling of metallic chips [18]. In work [19], it is shown that such process can provide significant improvements in environmental impact compared with conventional recycling. At the moment, friction stir extrusion technology is

* Corresponding author.
E-mail address: livan.fratini@unipa.it (L. Fratini).

https://doi.org/10.1016/j.cirp.2025.03.042
0007-8506/© 2025 The Author(s). Published by Elsevier Ltd on behalf of CIRP. This is an open access article under the CC BY license (http://creativecommons.org/licenses/by/4.0/)

demonstrating high-quality wire drawing with aluminum and magnesium alloys, while the authors of [20] declare also a high potential for harder alloys. In this regard, by the combination of friction stir extrusion and friction-based additive manufacturing, it can be possible to implement a closed-loop industrial symbiosis approach based on the "Reuse of production waste within the same company" [21]. This paper aims to experimentally establish the possibility of using a two-step process approach consisting of friction stir extrusion and friction stir extrusion-based additive manufacturing, allowing the recycling of AA6082 heat-treatable aluminum alloy chips in a unique and "circular" production cycle.

2. Materials and methods

2.1. Friction stir extrusion of wire

The first step of the hybrid route is the production of the wire to be fed during the deposition step by means of Friction Stir Extrusion. The FSE process has been carried out on the dedicated Friction Stir Welding machine ESAB Legio 3ST For this purpose, the extrusion die was fixed on the working table of the equipment and filled with the AA6082 chips (Fig. 1(a), step 1). Before the process, the chips were degreased and pre-compacted by the FSE tool with a loading force of about 5 kN. The process was performed using the loading force ***F*** of 18.0 kN and the rotation speed ω of 600 rpm, based on previous experimental tests [16]. The tool used in the experiment was designed to provide the extrusion of 2.5 mm diameter wires with an extrusion ratio of 10.0. Wire lengths of 900 mm were obtained for each test. This length of the wire is the maximum achievable value using the current laboratory set-up. Then the extruded wires were used as a feedstock for the additive manufacturing process in the as-built state without any post-processing.

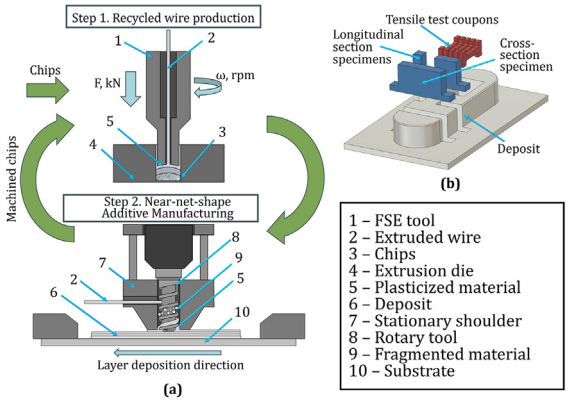

Fig. 1. (a) Schematic illustration of the industrial symbiosis link between friction stir extrusion-based additive manufacturing scrap and friction stir extrusion; (b) schematic of specimen cutting.

2.2. FSE-based additive manufacturing

For the implementation of Friction Stir Extrusion-based Additive Manufacturing (FSE-AM), a special tool was used, consisting of stationary and rotary parts, as shown in Fig. 1(a), step 2. Concerning the FSE, the process was performed using the ESAB Legio welding machine. The tool rotary part is characterized by 3.0-mm-thick threads with a pitch of 8.0 mm, and three pins with a length of 2.0 mm at the bottom. The stationary shoulder external diameter is 30.0 mm, and the gap between the internal diameter and the rotary tool diameter was set as 2.0 mm (1.0 mm in radius) to avoid frictional contact between the two parts.

The additive manufacturing process was performed as follows. The tool, with the specified rotation speed, started the plunge into the substrate to achieve the working position. When the position was reached, the dwell time was initiated, during which the feedstock was started to be fed into the cochlea to plasticize the wire material before the start of the tool movement. After the dwell time, the deposition process was started by assigning a travel speed to the tool to create one layer of material. Then, the tool was set back to the starting position on X-axis, while Z-axis starting point is increased by the previous layer thickness to deposit a new layer.

As the main process parameters, plunge depth ***h*** of −0.8 mm relative to the substrate face surface, dwell-time ***t*** of 4.0 s, tool travel speed ***V*** of 380 mm/min, and tool rotation speed ω of 1800 rpm were selected during the preliminary experimental campaign to reach enough level of material plasticization and provide stable layer formation process without visible defects. A 3.0-mm-thick substrate made of AA2098 aluminum alloy was used for the process. It is worth noting that the choice of a different aluminum alloy for the backplate was made to better highlight the occurring material flow and process mechanics, as detailed in Section 2.3. For each specimen, five layers with a length of 80 mm were deposited.

2.3. Structure analysis and mechanical testing

Specimens for metallographic analysis and tensile test coupons were cut out using electrical discharge machining. For metallography purposes, specimens were cut out in cross-sections and longitudinal sections to reveal the structure formation pattern (Fig. 1(b)). After cutting, they were subjected to standard preparation including polishing using 1.0 µm diamond suspension. Polished surfaces were chemically etched by Weck's reagent (100 mL H_2O, 1 g NaOH, 4 g $KMnO_4$) to reveal the grain structure of the used AA6082 aluminum alloy. The analysis of the material structure was performed using an optical microscope Olympus GX51 and a scanning electron microscope Phenom ProX Desktop. The same specimens were used for microhardness measurement. The tests were performed using Remet HBV-30A equipment with a loading of 500 g and a penetration time of 15 s. Measurements were conducted throughout the height of the cross-section with a step size of 0.5 mm. For wire hardness measurement, the tests were performed on a single cross-section with one indentation in the center and 4 indentations 250 µm off center. In the longitudinal section, it was measured throughout the 10 mm length with a pitch of 0.5 mm. After that, the average values were calculated. For tensile testing, test coupons were cut out in an XZ-plane with a gauge length of 10.0 mm, width of 2.7 mm, and thickness of 1.9 mm. Testing was carried out using a universal testing machine Galdabini Quasar 600 with a crosshead speed of 1 mm/s.

3. Results and discussion

3.1. FSE recycled wire

As a result of the first step of the proposed hybrid method, recycled wires made of AA6082 aluminum chips were produced. In Fig. 2, the longitudinal section of the recycled wire is shown. It is visible that the wire is fully dense and has no defects. The grain size of the wire was measured. It was found that after the extrusion process, the microstructure of the wire is represented by fine and almost equiaxed grains with an average size of 4.4 ± 1.7 µm.

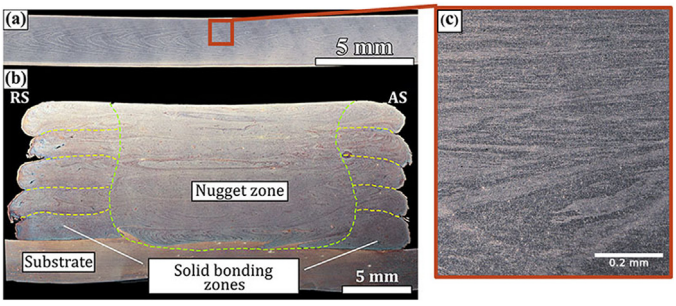

Fig. 2. (a) Macrostructure of recycled AA6082 wire in longitudinal section, (b) upcycled FSE-AM sample in cross-section, and (c) microstructure of wire.

Microhardness measurements showed that the mechanical properties of the wire have a quite small anisotropic behavior. It was observed that in the cross-section the average Vickers hardness is 65 ± 3.1 HV. At the same time, in the longitudinal section, i.e. along the extrusion axis, the measured value is 60 ± 1.8 HV, with a decrease of about 8 %. The hardness of the processed material is slightly lower than that for the T4 state of the AA6082 alloy (65 HV), but higher than for the AA6082-O alloy (35 HV). This behavior is caused by the thermomechanical action of the FSE-tool, leading to creating a new alloy "temper" due to severe plastic deformation and dynamic recrystallization [17].

3.2. FSE-AM: structure formation

Using the recycled wires, a build consisting of 5 layers was deposited using the FSE-AM method. In Fig. 2(b), the macrostructure of the as-built sample is shown. It is visible from the figure that the top surface of the build is flat enough and has no visible defects, while the edges, namely the solid bonding zones of the sample, have irregularities. These irregularities are related to the layer-by-layer deposition process and may be accompanied by lack of bonding defects and/or voids. When their size is small enough and they are positioned in the periphery of the build (which will undergo final machining) the main body of the sample can be considered sound. Due to the presence of tool pins, the center of the sample is not just bonded but stirred. This results in the formation of several consecutive nuggets in the central area of the build, indicated as nugget zone in Fig. 2.

The longitudinal section of the sample shows the material flow patterns along the build direction (Fig. 3). It is visible that in the solid bonding zone, the deposition process faces material flow inhomogeneity on the top of the sample. This results in the formation of a void observed in the fourth layer, as shown in Fig. 3(b). Due to the presence of pins penetrating the substrate, i.e. the previously deposited layer, in the nugget zone the layer boundaries moved down with respect to the bonding zones (Fig. 3(a)).

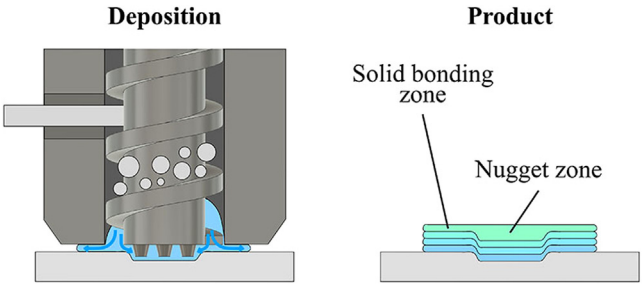

Fig. 3. Longitudinal section of as-built AA6082 FSE-AM sample in the (a) nugget zone and (b) solid bonding zone.

The layers formed in the nugget zone have a more regular shape with clearly visible layered structure characteristic for pin-induced material transfer in friction stir welding [22]. Additionally, for the first layer, part of the copper of the AA2098 substrate is visible, indicating significant material mixing. However, while the same set of process parameters was used for each layer, when depositing top layers, hotter material is found in the substrate resulting in higher process temperature. An in-depth analysis of process parameter effects and layer-dependent optimization will be performed in future work. Based on structural features observed in Figs. 2 and 3, the schematic illustration of layer formation macro-mechanism during FSE-AM is suggested (Fig. 4). First, the tool pins plunge into the previously deposited layer or substrate by the specific plunge depth forming a gap between the shoulder and a substrate which must be filled by a new layer. Then, with simultaneous wire feeding and tool travel, the material goes true fragmentation and plasticization. The plasticized material fills this gap being transferred to the edge, forming the solid bonding zone, and stirred by the pins, creating a nugget. As a result, the T-shaped layer is formed with flat top-surface, solid bonding zones on edges, and the nugget zone deepened into the previous layer

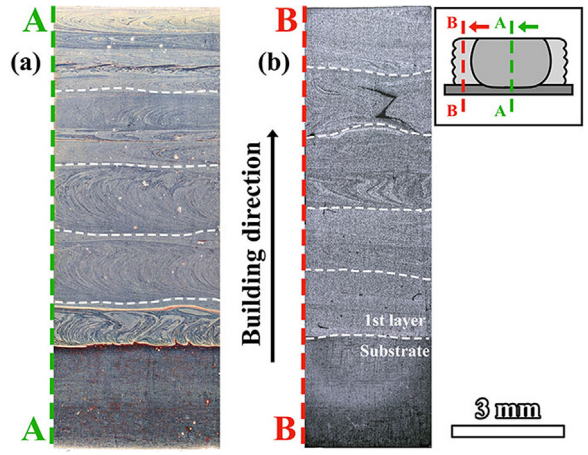

Fig. 4. Schematic illustration of layer formation macro-mechanism during FSE-AM in cross-section.

by pin plunge. It must be noted that due to the high temperatures, pressures, and frictional forces, the tool wear can appear as it was shown for related technologies like FSW [23], resulting in some changes in material transfer. However, this was not considered in this study.

The grain structure of the sample is shown in Fig. 5(a). The microstructure is represented by equiaxial grains with an average size of 4.9 ± 1.65 μm and different secondary phase particles. The main body of the deposit contains coarse particles of α-Al(FeMn)Si secondary phase and ultrafine precipitates of β"-Mg_2Si phase. Inside the nugget zone, onion rings consisting of different material flows are visible. It is observed that, throughout the height of the build, copper-rich areas consisting of Al_7Cu_2Fe particles are detected by EDS-analysis (Figs. 5 and 6 (b, c)). This behavior relates to the stirring of the substrate material with the first layer of deposit. In this way, some part of AA2098 alloy was adhered to the steel tool surface and transferred during the deposition of subsequent layers.

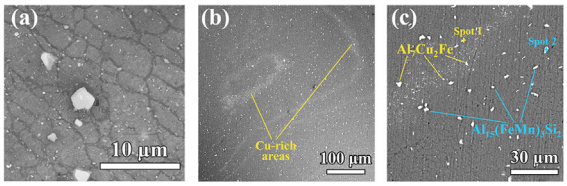

Fig. 5. Microstructure of AA6082 sample nugget illustrating (a) grain structure and intermetallic particles, (b) different material flows, and (c) the particles inside these flows.

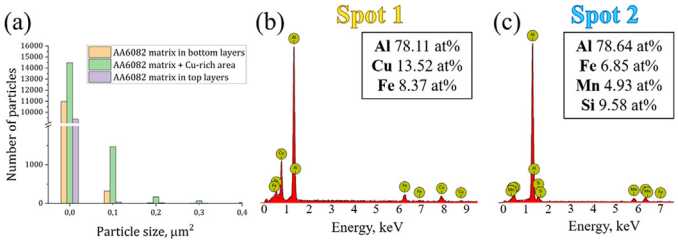

Fig. 6. (a) Size distribution of particles in the nugget zone of AA6082 FSE-AM sample, and EDS-analysis results of (b) spot 1 and (c) spot 2 shown in Fig. 5.

It was found that in the parts not affected by substrate material intermixing, the fine Mg_2Si particles prevail in the structure, while the fraction of coarse precipitates is quite low (Fig. 6). At the same time, in Cu-rich areas, the total volume fraction of particles is higher than in the AA6082 matrix (5.2 % and 3.4 %, respectively). Moreover, a large number of coarse particles of the Al-Cu-Fe system can be found in such regions.

A noticeable difference in particle size is also observed between the top and bottom of the sample. It is well known that precipitation of fine Mg_2Si particles is affected by the aging temperature and duration, resulting in the coarsening of particles at longer times.

Considering that friction stir-based processes are characterized by specific thermo-mechanical action, successive aging occurs in bottom layers during multi-layer deposition. At the same time, fine particles of Mg_2Si phase, responsible for dispersion hardening of the alloy, predominate in top layers that do not undergo re-heating.

3.3. FSE-AM: mechanical properties

Microhardness measurement results show a non-homogeneous distribution (Fig. 7(a)). For approximately 2/3 of the sample height, the microhardness is equal to about 55 HV, which is 13 % lower than the wire material and 18 % lower than AA6082-T4. However, HV gradually increases towards the top of the sample, reaching a maximum of about 80 HV. This value is 23 % higher than AA6082-T4 alloy HV and 28 % higher than recycled wire. This result can be explained by the thermal history during the manufacturing process. When a new layer is deposited, previous ones are repetitively heat affected, leading to over-aging of the material [24]. As a result of over-aging, there is a coarsening of intermetallic particles revealed in Section 3.2, especially Mg_2Si dispersoids. In turn, the coarsening leads to a weakening of the alloy. This effect can probably be eliminated by adjusting the rotation speed to maintain constant process temperature with the increasing number of layers, for a given dwell time between layers, i.e. without affecting process productivity and deposition rate.

Tensile test results show that, consistently with HV results, ultimate tensile strength (UTS) values are in a range between the UTS of the parent material in the O and T4 conditions (Fig. 7(b)). The UTS of FSE-AM material in the nugget zone is about 175 MPa with relative elongation at break of about 23 %. In the solid bonding zones, UTS reaches 172 MPa on the advancing side and 163 MPa on the retreating side with ductility of 15 % in both cases. Such mechanical behavior relates to different structure formation mechanisms in the nugget zone and solid bonding zones leading to reduced properties on the edges. It should be noted that while the UTS values are lower than the ones of AA6082-T4, the deposited material demonstrates higher ductility in the nugget zone.

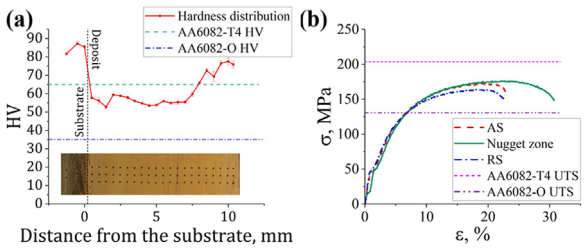

Fig. 7. (a) Microhardness distribution of the AA6082 sample in the cross-section and (b) stress-strain curves obtained by uniaxial tensile testing of AA6082 alloy in advancing side (AS), retreating side (RS) [25] and nugget zone of additive sample.

4. Comparison with existing processes

Due to the possibility of production of full-dense feedstock by FSE and its utilization by FSE-AM, this method opens possibilities not available with its competitors such as AFSD and WAAM. The comparative data, reported in table 1, indicates that FSE-AM technology is the only known method allowing the use of heat-treatable aluminum alloys with robotic AM deposition set-up for large-scale manufacturing [26], providing very high process flexibility using unique equipment for all the production stages. However, it is now only proved for operating with aluminum alloys, while WAAM already has possibilities for 3D-printing with titanium, steel, and other high-strength materials.

Concerning the environmental performance, the advantage of the here proposed FSE-AM goes beyond the use of chips as feedstock, as some benefits also lie in the deposition step. The preliminary energy input measurements carried out proved that the specific energy input of the FSE-AM is comparable to that measured for the AFSD [16] and it is much lower than the energy required by the WAAM. It is worth mentioning that the higher energy input of WAAM is mainly caused by the specific embodied energy of the shielding gas (57.4 MJ/kg [5]). In turn, for the FSE-AM and the AFSD the specific energy input is made only of electrical energy consumption as no consumables are needed. Also, the first deposition rate measurements reveal that the FSE-AM approach allows higher productivity as compared to the other technologies. Finally, it is worth remarking that, being these technologies in their early-stage development, dedicated machine development is needed to further improve their energy efficiency.

Table 1
Comparative analysis of additive manufacturing technologies for heat-treatable aluminum alloys

Feature	FSE-AM	AFSD [16]	WAAM [5]
Heat-treatable AA	+	+	–
High-strength materials (Titanium, Steel)	–	–	+
Chips based feedstock	+	+	Improvement needed [27]
Robotic setup capability	+	–	+
End-to-end equipment utilization	+	–	–
Deposition rate, kg/h	1.51	0.76	1.10
Specific Energy Input, MJ/kg	18.5	16.7	8.8 + 57.4

5. Conclusions

This study investigated the feasibility of a friction stir extrusion-based additive manufacturing approach for heat-treatable aluminum alloys.

The results obtained in this study show a high level of suitability of the process for recycling heat-treatable aluminum alloys, although some small defects were observed on the edges of the sample. As regards the microstructure, an effect of the thermal history, resulting in over-aging of as-built material, is noted. As a result, the mechanical properties of the FSE-AM material are in the mid-range between O and T4 temper of AA6082 alloy. However, this can likely be improved by subsequent heat treatment as was suggested for other AM methods and FSW-based processes.

Among the competitive methods, the proposed method demonstrates multiple advantages from both a technological and environmental point of view with respect to both AFSD and CMT-WAAM. In this way, the studied approach showed high suitability for the closed-loop industrial symbiosis implementation by in-house recycling of aluminum chips.

Declaration of competing interest

The authors declare that they have no known competing financial interests or personal relationships that could have appeared to influence the work reported in this paper.

CRediT authorship contribution statement

Kirill Kalashnikov: Writing – original draft, Validation, Investigation, Formal analysis. **Davide Campanella:** Validation, Investigation, Formal analysis. **Giuseppe Ingarao:** Writing – review & editing, Project administration, Conceptualization. **Gianluca Buffa:** Writing – review & editing, Project administration, Conceptualization. **Livan Fratini:** Supervision, Conceptualization. **Fabrizio Micari:** Supervision.

Acknowledgment

This study was carried out within the activity of project: “Aluminum Low Impact Circular Economy (ALICE)”, funded by the European Union - Next Generation EU, Mission 4 Component 1, Project ID: P2022WN727, CUP: B53D23027340001 PRIN 2022-PNRR.

References

[1] MINING.COM. All the metals we mined in one visualization. https://www.mining.com/web/all-the-metals-we-mined-in-one-visualization-2/ (Accessed November 15, 2024).
[2] Georgantzia E, Gkantou M, Kamaris GS (2021) Aluminium alloys as structural material: a review of research. *Engineering Structures* 227:111372.
[3] DebRoy T, Wei HL, Zuback JS, Mukherjee T, Elmer JW, et al. (2018) Additive manufacturing of metallic components – Process, structure and properties. *Prog Mater Sci* 92:112–224.
[4] Kumar M, Gibbons GJ, Das A, Manna I, Tanner D, et al. (2021) Additive manufacturing of aluminium alloy 2024 by laser powder bed fusion: microstructural evolution, defects and mechanical properties. *Rapid Prototyp J* 27/7:1388–1397.
[5] Campatelli G, Campanella D, Barcellona A, Fratini L, Grossi N, et al. (2020) Microstructural, mechanical and energy demand characterization of alternative WAAM techniques for Al-alloy parts production. *CIRP Journal of Manufacturing Science and Technology* 31:492–499.
[6] Klein T, Arnoldt A, Lahnsteiner R, Schnall M (2022) Microstructure and mechanical properties of a structurally refined Al–Mg–Si alloy for wire-arc additive manufacturing. *Materials Science and Engineering: A* 830:142318.
[7] Pan Y, Yu M, Xu C, Zhang J, Geng L (2024) High-performance 2319 aluminum alloy via CMT-WAAM: microstructure, porosity, and mechanical properties. *Metals (Basel)* 14/7:797.
[8] Sarıkaya M, Başcıl Önler D, Dağlı S, Hartomacıoğlu S, Günay M, et al. (2024) A review on aluminum alloys produced by wire arc additive manufacturing (WAAM): applications, benefits, challenges and future trends. *Journal of Materials Research and Technology* 33:5643–5670.
[9] Liu FC, Feng AH, Pei X, Hovanski Y, Mishra RS, et al. (2024) Friction stir based welding, processing, extrusion and additive manufacturing. *Prog Mater Sci* 146:101330.
[10] Shao J, Samaei A, Xue T, Xie X, Guo S, et al. (2023) Additive friction stir deposition of metallic materials: process, structure and properties. *Mater Des* 234:112356.
[11] Seidi E, Miller SF, Carlson BE (2021) Friction surfacing deposition by consumable tools. *Journal of Manufacturing Science and Engineering* 143/12.
[12] Chen H, Meng X, Chen J, Xie Y, Wang J, et al. (2023) Wire-based friction stir additive manufacturing. *Additive Manufacturing* 70:103557.
[13] Rezaeinejad SS, Strik DH, Visser RM, Bor TC, Luckabauer M, et al. (2023) Solid-State additive manufacturing of AA6060 employing friction screw extrusion additive manufacturing. *JOM* 75/10:4199–4211.
[14] Bor T, Leede Mde, Deunk F, Lind J, Lievestro W, et al. (2023) Friction screw extrusion additive manufacturing of an Al-Mg-Si alloy. *Additive Manufacturing* 72:103621.
[15] Haridas RS, Gumaste A, Varshney P, Manu BR, Kandasamy K, Kumar N, et al. (2023) SolidStir additive manufacturing: a novel deformation-based additive manufacturing using friction stir technology. *JOM* 75:4231–4241.
[16] Yoder JK, Hahn GD, Zhao N, Brennan RE, Cho K, et al. (2023) Additive friction stir deposition-enabled upcycling of automotive cast aluminum chips. *Additive Manufacturing Letters* 4:100108.
[17] Buffa G, Campanella D, Adnan M, La Commare U, Ingarao G, et al. (2024) Improving the industrial efficiency of recycling aluminum alloy chips using friction stir extrusion: thin wires production process. *International Journal of Precision Engineering and Manufacturing-Green Technology* 11/4:1133–1146.
[18] Laurent-Brocq M, Lilensten L, Pinot C, Schulze A, Duchaussoy A, Bourgon J, et al. (2023) Solid state recycling of aluminium chips: multi-technique characterization and analysis of oxidation. *Materialia* 31:101864.
[19] Duflou JR, Tekkaya AE, Haase M, Welo T, Vanmeensel K, Kellens K, et al. (2015) Environmental assessment of solid state recycling routes for aluminium alloys: can solid state processes significantly reduce the environmental impact of aluminium recycling? *CIRP Annals* 64:37–40.
[20] Akbari M, Asadi P, Behnagh RA, Bedir F, Choupani N, Sadowski T (2025) Process parameters and tool design in friction stir extrusion: a sustainable recycling technique. *Engineering Reports* 7:e13060.
[21] Duflou JR, Wegener K, Tekkaya AE, Hauschild M, Bleicher F, et al. (2024) Efficiently preserving material resources in manufacturing: industrial symbiosis revisited. *CIRP Annals* 73/2:695–721.
[22] Kalashnikova T, Chumaevskii A, Kalashnikov K, Fortuna S, Kolubaev E, et al. (2020) Microstructural analysis of friction stir butt welded Al-Mg-*Sc*-Zr alloy heavy gauge sheets. *Metals (Basel)* 10/6:806.
[23] Tarasov SYu, Rubtsov VE, Kolubaev EA (2014) A proposed diffusion-controlled wear mechanism of alloy steel friction stir welding (FSW) tools used on an aluminum alloy. *Wear* 318:130–134.
[24] Kalashnikov KN, Tarasov SY, Chumaevskii AV, Fortuna SV, Eliseev AA, et al. (2019) Towards aging in a multipass friction stir–processed *AA*2024. *The International Journal of Advanced Manufacturing Technology* 103/5–8:2121–2132.
[25] Khan N, Rathee S, Srivastava M (2021) Friction stir welding: an overview on effect of tool variables. *Materials Today: Proceedings* 47:7196–7202.
[26] Zhang Z, Wan L, Meng X, Xie Y, Tian H, et al. (2024) Robotic wire-based friction stir additive manufacturing. *Additive Manufacturing* 88:104261.
[27] Carvalho GHSFL, Campatelli G, Fratini L (2024) Feasibility study of using friction stir extruded recycled aluminum rods for welding and additive manufacturing. *Manufacturing Letters* 42:52–55.